

Resonances of individual metal nanowires in the infrared

F. Neubrech, T. Kolb, R. Lovrincic, G. Fahsold, and A. Pucci^{a)}
Kirchhoff-Institut für Physik, University of Heidelberg, INF 227, D-69120 Heidelberg, Germany

J. Aizpurua
Donostia International Physics Center, Donostia-San Sebastian 20018, Spain

T. W. Cornelius, M. E. Toimil-Molaes, and R. Neumann
Gesellschaft für Schwerionenforschung (GSI), Planckstr. 1, D-64291 Darmstadt, Germany

S. Karim
Fachbereich Chemie, University of Marburg, Hans-Meerwein-Str., D-35032 Marburg, Germany

(Received 2 August 2006; accepted 9 November 2006; published online 18 December 2006)

With infrared spectroscopic microscopy using synchrotron light, the authors studied resonant light scattering from single metal nanowires with diameters in the 100 nm range and with lengths of a few microns. The Au and Cu nanowires were electrochemically grown in polycarbonate etched ion-track membranes and transferred on infrared-transparent substrates. Significant antennalike plasmon resonances were observed in good agreement with exact light-scattering calculations. The resonances depend not only on length and diameter but also on the dielectric surrounding of the nanowire. The observed maximum extinction at resonance corresponds to an electromagnetic far-field enhancement by a factor of about 5. © 2006 American Institute of Physics.

[DOI: 10.1063/1.2405873]

Nanosized metal objects exhibit interesting optical properties with numerous applications in technology and life science,¹⁻⁴ for example, their surface plasmon resonance surface plasmon resonances that can be exploited to confine electromagnetic radiation to a volume of subwavelength dimensions.⁵ The potential of nanosilts in gold nanorods for high optical near field enhancement has been reported recently.⁶ In the infrared (IR), field enhancement due to resonances of nanoantennas should be especially high due to (i) the strong negative part of the metal dielectric function and (ii) the high aspect ratio. Via surface enhanced IR absorption (SEIRA)^{7,8} field enhancement should enable the detection of vibrational fingerprints of single molecules on nanoantennas by studying light scattering with apertureless scanning near field microscopy.⁹

In general, the frequency of the resonance of a metal nanoparticle depends not only on the kind of metal but also on shape and size. Going from spherical particles to prolate spheroids, the shape dependence becomes increasingly important. The fundamental plasmon resonance splits into two branches with one low-energy plasmon mode. The larger is the length ratio of the long axis of the particle to the short one, the lower the frequency of this mode. Hence, metal nanowires with lengths above a certain value exhibit resonances in the IR range.¹⁰ If the length of the wire is in the range of the exciting wavelength, effects from retardation dominate the resonance condition. The limited speed of light gives rise to a direct dependence of the resonance on the absolute size of the object. This is well known from purely classical theory of scattering of electromagnetic waves by (ideal) metal objects, where antenna resonances occur if the length L of a thin linear wire matches with multiples of the wavelength λ ,

$$L = m\lambda/(2n), \quad (1)$$

with m a natural number and n the refractive index of the surrounding medium. The fundamental (or main) resonance is represented by $m=1$. Higher m values correspond to dipolelike excitations along the antenna axis only for odd m . Nevertheless, excitations at even m may be detected if any electric field vector is oblique to the main wire axis,¹¹ or for bent wires. If the diameter D of the wires is not negligible compared to the wavelength, both resonance frequency and line shape depend also on D . Thus classical antenna theory¹² predicts that for nanowires with the same length L , the smaller the aspect ratio L/D , the more broadened the resonance and the lower the resonance frequency. In the case of nanowires, also the skin effect plays an important role, since the skin thickness may be of the diameter's order of magnitude. The skin effect introduces both the dependence on the antenna material and the qualitative change of the resonance conditions. For example, up to $L \approx 2 \mu\text{m}$, the approximate relation $L = \lambda/3$ for the fundamental resonance of gold nanowires with $D=40$ nm and hemispherical tip ends was theoretically found.⁶ With increasing D , this relationship shifts towards the result from relation (1); the diameter dependent influence of the skin effect on the resonance condition is opposite to the geometrical one. In addition, the polarizability of the surrounding medium is important for the optical properties of metal nanostructures.¹³ Usually, to describe the substrate effect on optical spectra of metal nanoparticles, an effective dielectric constant

$$\epsilon_{\text{eff}} = (1 + n_s^2)/2 \quad (2)$$

is assumed as embedding the particle completely (n_s is the refractive index of the substrate).¹⁴

This letter reports on the experimental investigation of the antennalike plasmon resonances of single metal nanowires (supported by a dielectric substrate) in the IR. Compared to previous studies performed on nanowire ensembles,¹⁰ single nanowire measurements exclude the in-

^{a)} Author to whom correspondence should be addressed; electronic mail: pucci@kip.uni-heidelberg.de

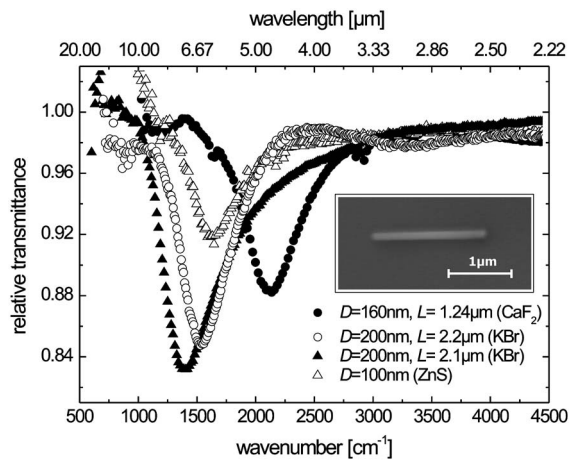


FIG. 1. Selection of relative IR transmittance spectra of various individual wires with different lengths L and diameters D on different substrates. The inset shows a scanning electron microscopy image of a gold nanowire with $L=1.7 \mu\text{m}$ and $D=100 \text{ nm}$.

fluence of wire-wire interactions and overcome the necessity of averaging over locally varying parameters. These two facts allow us to compare our experimental results with existing theories.

Cu and Au nanowires with diameters between 100 and 200 nm have been prepared by electrochemical deposition in etched ion-track polycarbonate membranes.^{15–17} After fabrication, the polymer membrane was dissolved in dichloromethane. The clean wires were then placed onto an IR transparent substrate (e.g. KBr, $n_s=1.53$). During the sample preparation process, the wires break into pieces with lengths between several hundred nanometers and several micrometers (and with undefined tip ends). Due to specific deposition parameters, Au nanowires were polycrystalline,¹⁵ and Cu nanowires consisted of long single-crystalline sections.¹⁷

IR spectroscopy of single nanowires was performed at the IR beamline of the synchrotron light source ANKA at the Forschungszentrum Karlsruhe. First, the wire length was determined by microscopy with visible light (which gives an error of up to 8%). Then, with a circular aperture, we selected an area with a diameter of $8.3 \mu\text{m}$ in the focal plane of the microscope (Bruker IIRscope II) and centered it on a single nanowire for the IR transmittance measurement and subsequently, for taking the reference measurement, placed it at least $10 \mu\text{m}$ away from any nanowire. The spectroscopic measurements were done with a Fourier-transform IR spectrometer (Bruker IFS 66 v/S). A LN₂-cooled mercury cadmium telluride detector collects the light normally transmitted through the sample area. Since the collection lens has a numerical aperture of 0.52, a small part of light scattered away from the normal direction could be also detected. However, as in Ref. 10, most of the power scattered by the antenna goes to directions outside the cone of collected light. IR spectra were taken each by acquisition of at least ten scans in the spectral range from 600 to 5000 cm^{-1} and with resolution of 16 cm^{-1} . An IR polarizer was inserted in the optical path before the sample.

The relative transmittance T_{rel} (ratio of transmittance of the substrate area with and without wire, see Fig. 1) revealed fundamental antenna resonances. As expected, resonances were strongly polarization dependent and were observed only for electrical field parallel to the long wire axis. All spectra shown here belong to this kind of polarization. For

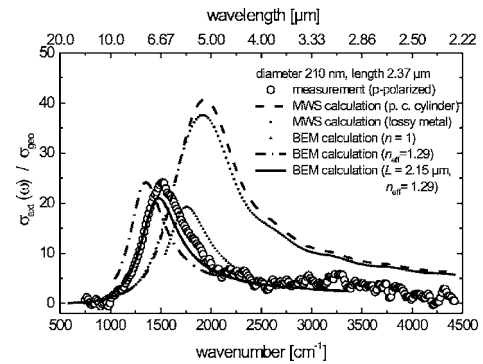


FIG. 2. Extinction cross section (relative to geometric cross section) of a gold nanowire ($L=2.37 \mu\text{m}$, $D=210 \text{ nm}$): experimental data, calculations with MWS for perfect conducting (p.c.) cylinder and for lossy metal with dc conductivity of $4.09 \times 10^7 \text{ S/m}$, calculations with BEM for wire in vacuum ($n=1$), wire in medium with $n_{\text{eff}}=1.29$ (dash-dotted curve), and for $L=2.15 \mu\text{m}$ and $n_{\text{eff}}=1.29$ (full line).

polarization perpendicular to the wire axis, the IR signal was below the noise level.

From normal transmittance measurements the ratio of the extinction cross section σ_{ext} of a single nanowire to its geometric cross section σ_{geo} can be estimated. We use the relation

$$\sigma_{\text{ext}}/\sigma_{\text{geo}} = A_0(1 - T_{\text{rel}})(n_s + 1)(2LD)^{-1} \quad (3)$$

that follows from $1 - T_{\text{rel}} \approx (\sigma_{\text{ext}}/A_0)2/(n_s + 1)$, where the refractive index n_s of the substrate is taken into account in analogy to the normal transmittance change by the substrate of a thin film¹⁸ compared to a freestanding film.¹⁹ That substrate effect leads to a decreased film signal, particularly in case of high n_s . Inserting A_0 as the spot size of the IR microscope, n_s for the relevant substrate, L (from VIS microscopy), and D (known from the wire-growth process) gives $\sigma_{\text{ext}}/\sigma_{\text{geo}}$ in Fig. 2. Any result >1 means an extinction of intensity above simple shadowing, which indicates local-field enhancement in the vicinity of the nanowire. Since we measure in the far field we obtain the spatially averaged field-enhancement factor $\sqrt{\sigma_{\text{ext}}/\sigma_{\text{geo}}}$. The experimental data of Fig. 2, that are representative for most of our experiments, correspond to $\sqrt{\sigma_{\text{ext}}/\sigma_{\text{geo}}} \approx 5$ at the resonance maximum. The calculated curves in Fig. 2 are based on the assumption of rods with hemispherical tip ends. Those marked by “MWS calculation” are modeled with the software MICROWAVE STUDIO (Ref. 20) (MWS) for antenna problems. In these finite-element calculations we described the metal as perfectly conducting (“pc cylinder”) or as a “lossy” one, respectively; both approximations neglect the imaginary part of the conductivity. But the “lossy metal” model takes into account the proper skin depth, i.e., a value close to that following from the Drude-type dielectric function.²¹ It is obvious that the skin depth has only a minor effect on the calculated spectrum because the wire is relatively thick. The resonance curves calculated with the exact boundary element method^{6,22} (BEM), including retardation and bulk complex material response, are in better agreement to the experiment. With BEM the near field enhancement factor at resonance is 30 for the wire from Fig. 2 in vacuum, involving a SEIRA effect similar to that found in complex metal nanostructures.⁸

The detailed differences in the metal properties of Au and of Cu are not significant for the resonance curve because

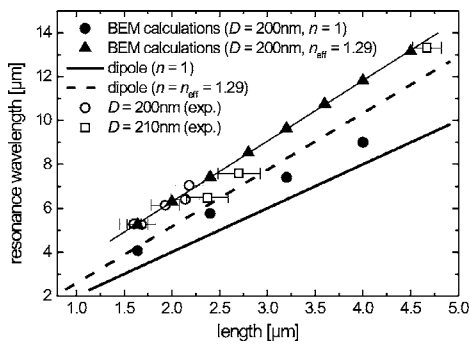


FIG. 3. Resonance wavelength vs wire length L for gold wires with similar D on KBr: experimental data, detailed calculations, and simple antenna model.

of the similar skin depths (22 nm for Au and 24 nm for Cu at 2000 cm^{-1})²³ regarding the much bigger D .

The substrate effect was only approximately included in the calculations: as an effective embedding medium with refractive index $n_{\text{eff}} = \sqrt{\epsilon_{\text{eff}}} = 1.29$ (for a KBr substrate) in two of the three BEM calculations. That calculation with the slightly changed wire length (within the experimental error) fits well to the experimental curve. The same does a calculation (not shown) with L unchanged and n_{eff} set to 1.20. The ambiguity in the theoretical resonance position due to the uncertainty in L produces a limitation in the exact determination of the very complex substrate effect.²⁴ But, looking at Fig. 3 where we compare experimental resonance data for wires with comparable diameters on KBr, not only a systematic deviation from simple antenna theory (lines) is obvious, the BEM calculation with consideration of the effective refractive index (full triangles) again yields reasonable agreement to experiment (open symbols). Calculations (not shown) for wires fully embedded in KBr give too high resonance wavelength.

To separately demonstrate the effect of polarizability of the surrounding medium we covered single nanowires with paraffin wax. As obvious in Fig. 4, the resonance is shifted to lower frequencies. Assuming the dependence on refractive index as given in Eq. (1), we obtain the ratio $n_{\text{eff}}^{\text{air}}/n_{\text{eff}}^{\text{paraffin}} = 0.90 \pm 0.03$ from the resonance frequencies before and after evaporating paraffin. This is in reasonable accord with 0.923 which follows from $\epsilon_{\text{eff}} = (\epsilon_m + n_s^2)/2$, compared to Eq. (2)

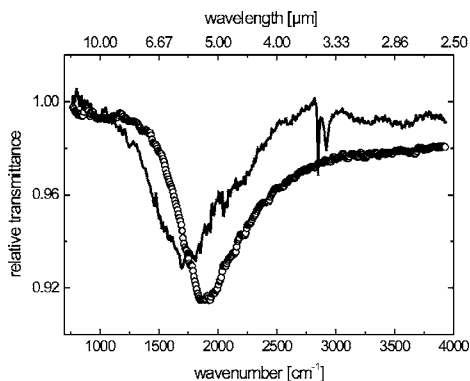


FIG. 4. Relative transmittance spectra of a bare gold wire (open circles) with $D=100\text{ nm}$ and $L=1.4\text{ }\mu\text{m}$ on ZnS and of the same wire covered with paraffin (full line). The reference for the paraffin-covered wire is paraffin-covered ZnS. From the paraffin layer, C-H stretching vibrations appear around 2900 cm^{-1} , which is due to inhomogeneous thickness.

with $n_s^2 = \epsilon_s = 4.84$ for ZnS (at $10\text{ }\mu\text{m}$) and $\epsilon_m = 2.02$ for paraffin. With another wire on a KBr substrate $n_{\text{eff}}^{\text{air}}/n_{\text{eff}}^{\text{paraffin}}$ is 0.875 (from ϵ_{eff}) and 0.89 ± 0.06 (from the spectral shift), respectively.

In summary, we studied the main antenna resonance of single nanowires with diameters larger than the skin depth in the IR. The resonance curve of such wires cannot be described as originating from an ideal antenna. Besides the wire length, not only the diameter but also the penetration depth of light into the wire determine the resonance spectrum. The resonance curve is further modified by the polarizability of the substrate and of cover layers. As a useful approximation, the linear interpolation of the dielectric constants of substrate and cover medium can be used to estimate an effective refractive index for the antenna surrounding.

The authors gratefully acknowledge technical support by M. Süpfle and helpful discussions with B. Gasharova and Y.-L. Mathis. Acknowledgements for financial support are: for the Heidelberg group from the DFG (DFG Fa432/7-1), for S.K. from Higher Education Commission Pakistan, for J.A. from the NANOTRON project.

¹S. Link and M. A. El-Sayed, *C. R. Math.* **103**, 8410 (1999).

²N. Féliidj, J. Aubard, G. Lévi, J. R. Krenn, M. Salerno, G. Schider, B. Lambrecht, A. Leitner, and F. R. Aussenegg, *Phys. Rev. B* **65**, 075419 (2002).

³G. Schider, J. R. Krenn, A. Hohenau, H. Ditlbacher, A. Leitner, F. R. Aussenegg, W. L. Schaich, I. Puscasu, B. Monacelli, and G. Boreman, *Phys. Rev. B* **68**, 155427 (2003).

⁴J. Grand, M. Lamy de la Chapelle, J.-L. Bijeon, P.-M. Adam, A. Vial, and P. Royer, *Phys. Rev. B* **72**, 033407 (2005).

⁵E. Cubukcu, E. A. Kort, K. B. Crozier, and F. Capasso, *Appl. Phys. Lett.* **89**, 093120 (2006).

⁶J. Aizpurua, Garnett W. Bryant, Lee J. Richter, F. J. García de Abajo, Brian K. Kelley, and T. Mallouk, *Phys. Rev. B* **71**, 235420 (2005).

⁷R. F. Aroca, D. J. Ross, and C. Domingo, *Appl. Spectrosc.* **58**, 324A (2004).

⁸D. Enders and A. Pucci, *Appl. Phys. Lett.* **88**, 184104 (2006).

⁹T. Taubner, R. Hillenbrand, and F. Keilmann, *Appl. Phys. Lett.* **85**, 5064 (2004).

¹⁰K. B. Crozier, A. Sundaramurthy, G. S. Kino, and C. F. Quate, *J. Appl. Phys.* **94**, 4632 (2003).

¹¹G. Laurent, N. Féliidj, J. Aubard, G. Lévi, J. R. Krenn, A. Hohenau, G. Schider, A. Leitner, and F. R. Aussenegg, *Phys. Rev. B* **71**, 045430 (2005).

¹²T. G. Ruck, *Radar Cross Section Handbook* (Plenum, New York, 1970), 1, 293–297.

¹³J. Mock, D. R. Smith, and S. Schultz, *Nano Lett.* **3**, 485 (2003).

¹⁴For example, M. M. Dvornenko, A. V. Goncharenko, V. R. Romaniuk, and E. F. Venger, *Physica B* **299**, 88 (2001).

¹⁵S. Karim, M. E. Toimil-Molares, F. Maurer, G. Miehe, W. Ensinger, J. Liu, T. W. Cornelius, and R. Neumann, *Appl. Phys. A: Mater. Sci. Process.* **84**, 403 (2006).

¹⁶J. Liu, J. L. Duan, M. E. Toimil-Molares, S. Karim, T. W. Cornelius, D. Dobrev, H. J. Yao, Y. M. Sun, M. D. Hou, D. Mo, Z. G. Wang, and R. Neumann, *Nanotechnology* **17**, 1922 (2006).

¹⁷M. E. Toimil-Molares, V. Buschmann, D. Dobrev, R. Neumann, R. Scholz, I. U. Schuchert, and J. Vetter, *Adv. Mater. (Weinheim, Ger.)* **13**, 62 (2001).

¹⁸U. Tschner and K. Huebner, *Phys. Status Solidi B* **159**, 917 (1990).

¹⁹D. W. Berreman, *Phys. Rev.* **130**, 2193 (1963).

²⁰cst Computer Simulation Technology, Darmstadt, Germany.

²¹M. A. Ordal, L. L. Long, R. J. Bell, S. E. Bell, R. R. Bell, R. W. Alexander, Jr., and C. A. Ward, *Appl. Opt.* **22**, 1099 (1983).

²²F. J. García de Abajo and A. Howie, *Phys. Rev. Lett.* **80**, 5180 (1998); *Phys. Rev. B* **65**, 115418 (2002).

²³G. Fahsold, M. Sinther, A. Priebe, S. Diez, and A. Pucci, *Phys. Rev. B* **65**, 235408 (2002).

²⁴V. Lozovski, *Physica E (Amsterdam)* **9**, 642 (2001).